J. Ocean Univ. China (Oceanic and Coastal Sea Research)
https://doi.org/10.1007/s11802-018-3353-9
ISSN 1672-5182, 2018 17 (2): 420-432
http://www.ouc.edu.cn/xbywb/
E-mail:xbywb@ouc.edu.cn

The Upper 1000-m Slope Currents North of the South Shetland Islands and Elephant Island Based on Ship Cruise Observations

DU Guangqian, ZHANG Zhaoru*, ZHOU Meng, ZHU Yiwu, and ZHONG Yisen

Institute of Oceanography, *Shanghai Jiao Tong University*, *Shanghai* 200240, *China*

(Received November 14, 2016; revised March 7, 2017; accepted March 7, 2017)

Abstract While the Antarctic Slope Current (ASC) has been intensively studied for the East Antarctica slope area and the Weddell Sea, its fate in the western Antarctic Peninsula (WAP) region remains much less known. Data from two cruises conducted near the South Shetland Islands (SSIs) and the Elephant Island (EI), one in austral summer of 2004 and one in austral winter of 2006, were analyzed to provide a broad picture of the circulation pattern over the continental slope of the surveyed area, and an insight into the dynamical balance of the circulation. The results indicate that southwestward currents are present over the upper slope in the study area, indicating the ASC in the WAP region. Near the Shackleton Gap (SG) north of the EI, the southwestward slope currents near the shelf break are characterized by a water mass colder and fresher than the ambient water, which produces cross-slope density gradients and then vertical shear of the along-slope (or along-isobath) velocity. The vertical shear is associated with a reversal of the along-slope current from northeastward at surface to southwestward in deeper layers, or a depth-intensification of the southwestward slope currents. The water mass with temperature and salinity characteristics similar to the observed cold and fresh water is also revealed on the southern slope of the Scotia Sea, suggesting that this cold and fresh water is originated from the Scotia Sea slope and flows southwestward through the SG. Over the shelf north of the SSIs, the cold and fresh water mass is also observed and originates mainly from the Bransfield Strait. In this area, vertical structure of the southwestward slope currents is associated with the onshore intrusion of the upper Circumpolar Deep Water that creates cross-slope density gradients.

Key words Antarctic Slope Current; dynamical balance; water masses; South Shetland Islands; Elephant Island

1 Introduction

The Antarctic continental slope is a crucial area for the formation of Antarctic Bottom Water, biogeochemical cycling and ecosystem functioning (Heywood *et al.*, 2014). A major physical feature over the slope area is the Antarctic Slope Current (ASC), which flows generally westward and connects the three major oceanic basins – the Pacific Ocean, the Atlantic Ocean and the Indian Ocean around Antarctica (Mathiot *et al.*, 2011; Peña-Molino *et al.*, 2016). It has been suggested that ASC might be circumpolar and not disrupted, so that it can affect the advection of nutrients and krill along the entire Antarctica (Heywood *et al.*, 2004; Quetin and Ross, 1984). Near the South Shetland Islands (SSIs), krill would lay eggs at depths of approximately 50 m, and the eggs can sink to depths of 800–1000 m before hatching (Quetin and Ross, 1984). Thus, eggs laid north of the SSIs may be transported westward towards the Bellingshausen Sea by these slope currents (Nowlin and Zenk, 1988).

Previous studies found that east of the Antarctic Peninsula, the Antarctic Slope Front, characterized by currents of about 20 cm s^{-1}, is split into three paths when it encounters the South Scotia Ridge: 1) turning west and flowing into the Bransfield Strait; 2) entrained in a large standing eddy over the South Scotia Ridge; and 3) following the 1000-m isobath very close to the Clarence Island on its eastern side, and leaving the Weddell Sea Confluence entering the Scotia Sea (Flexas *et al.*, 2015; Thompson *et al.*, 2009; Youngs *et al.*, 2015). A few studies have suggested a connection between the slope currents in the Scotia Sea and in the area north of the SSIs via the Shackleton Gap (SG), which is a passage over 3000 m deep and 30 km wide lying between the Shackleton Traverse Ridge (STR) and the Elephant Island (EI) (Heywood *et al.*, 2004; Locarnini *et al.*, 1993; Nowlin and Zenk, 1988). Based on conductivity-temperature-depth (CTD) measurements, Capella *et al*. (1992) found that west of the EI and north of the SSIs, a tongue of cold water extends southwestward along the shelf-edge from the EI to the Livingston Island. Nowlin and Zenk (1988) observed a persistent and narrow (with a width of 10 km)

* Corresponding author. Tel: 0086-21-34208062
E-mail: zrzhang@sjtu.edu.cn

bottom current flowing from the Weddell Sea westward into the Scotia Sea and further through the Drake Passage along the continental slope, with a mean velocity of 10 cm s^{-1}. They considered this westward deep slope component to be kinematically distinct from the upper slope/shelf current. With multiple years of shipboard Acoustic Doppler Current Profiler (ADCP) measurements, Savidge and Amft (2009) found southwestward currents near the shelf break north of the SSIs; nevertheless, the lack of hydrographic data in their study prevented them from further investigating the dynamical balance of these slope currents.

While these earlier studies have cast some light on the fate of slope currents west of the tip of the Antarctic Peninsula, detailed patterns of these currents remain largely unknown. The slope currents in the western Antarctic Peninsula (WAP) area should be an indispensable part of the circumpolar, anticyclonic ASC as researchers have previously assumed (*e.g.*, Heywood *et al.*, 2004), and should make significant contributions to water mass and heat transports, transports of nutrients and biota, life history of Antarctic krill connecting their spawning, nursing and mature sites, and ecosystem structure and dynamics in the WAP region (Nowlin and Zenk, 1988; Savidge and Amft, 2009; Siegel *et al.*, 2013). This study analyzed hydrographic and velocity data on eighteen transects in the slope regions north of the SSIs and the EI collected during an austral summer cruise in 2004 and an austral winter cruise in 2006, to obtain a better understanding of the structure and dynamics of the slope currents within the upper 1000 m of the water column in this area. Meanwhile, this study also employed historical shipboard ADCP measurements covering the WAP region to explore the persistence of all the slope currents on a long time scale.

2 Data and Methods

Datasets in the southern Drake Passage employed in this study were collected in an austral summer cruise conducted from 12 February to 24 March 2004 onboard the Antarctic Service and Research Vessel Laurence M. Gould (Zhou *et al.*, 2010; data are available at http://www.bco-dmo.org/deployment/58666), and an austral winter cruise conducted from 3 July to 15 August 2006 onboard the Ice Breaker Research Vessel Nathanial B. Palmer (Zhou *et al.*, 2013; data are available at http://www.bco-dmo.org/deployment/57976). The study area was bounded between 59°S and 65°S in latitude and between 64°W and 53°W in longitude, which covers the Ona Basin, the shelf and slope areas of the SSIs and the EI, the SG, and the southern STR (Figs.1b and c).

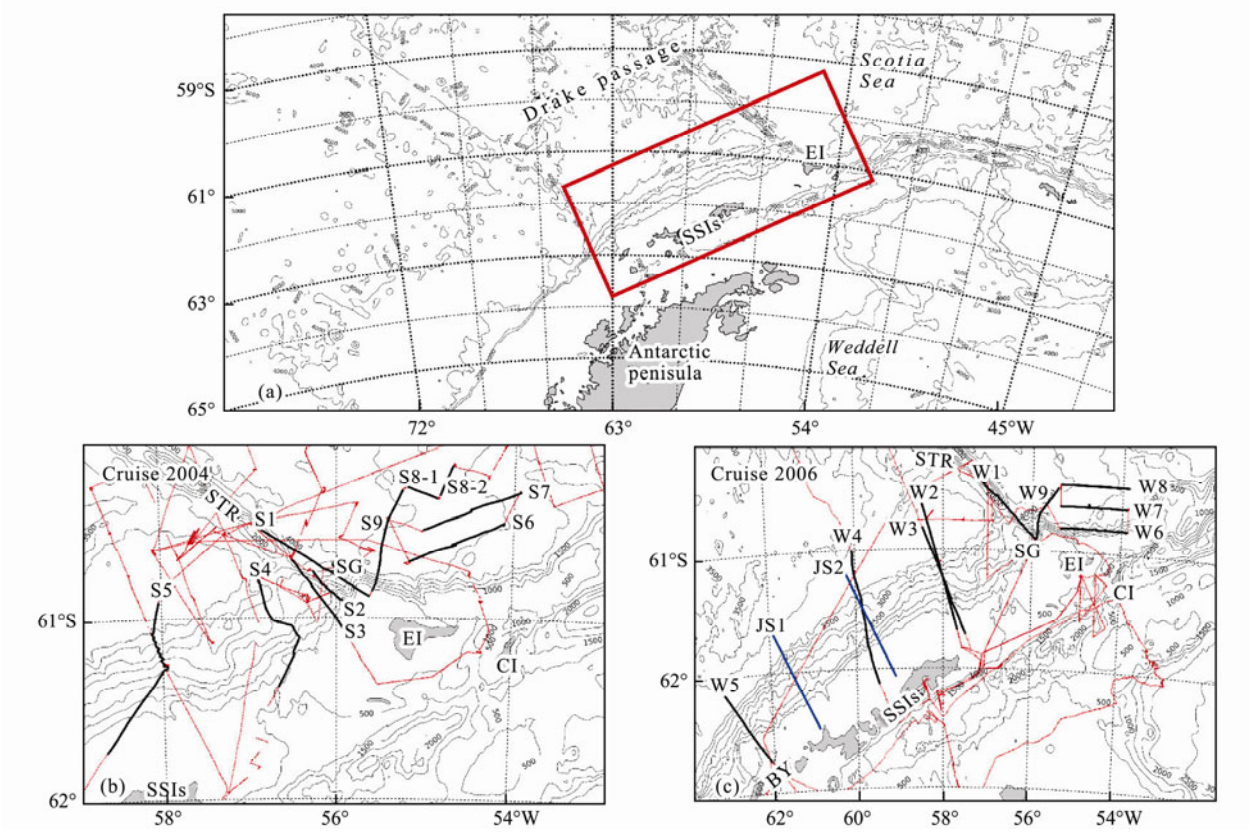

Fig.1 (a) Bathymetry in the southern Drake Passage with the study domain marked by the red box, (b) cruise tracks (red lines) and transects (black lines, S1–S9) during the 2004 austral summer cruise, and (c) cruise tracks (red lines) and transects (black lines, W1–W9) during the 2006 austral winter curises. The red dots in (b) and (c) represent stations covered by the cruises. The blue lines in (c) respresent the cross-slope transects (JS1 and JS2) used to analyze the JASADCP data. Depth contours shown (in m) are 0–7000 m by 1000-m increments in panel a, and 0–4000 m by 500-m increments in panel b and c. The abbreviations are Boyd Strait (BY), South Shetland Islands (SSIs), Elephant Island (EI), Clarence Island (CI), Shackleton Transverse Ridge (STR), and Shackleton Gap (SG).

A regular rosette system was used for collecting hydrography data in both the 2004 and 2006 cruises, which was equipped with a SeaBird 911 plus CTD system with dual temperature and conductivity sensors (Sea-Bird Electronics, Inc., Bellevue, WA, USA). All temperature and conductivity sensors were calibrated prior to the cruises. Throughout the entire cruises, the standard deviations between two pairs of temperature and salinity sensors were within 0.01℃ and 0.01, respectively, which validated the stabilities of the sensors. Most of the CTD casts were made to depths of 10 m above the bottom or 1000 m when the water depth is greater than 1000 m, except for some stations located on the slope of the Weddell Sea and the Scotia Sea.

Both of the 2004 and 2006 cruises were mounted with a vessel-mounted 153 kHz Narrow Band ADCP (RD Instruments, San Diego, CA, USA), which was used for direct current measurements. Both of the ADCPs were set with a bin length of 8 m, a pulse length of 8 m and a blank after transmission of 4 m. These settings led to a standard deviation of 13 cm s^{-1} for single ping velocity measurements (RDI, 1989). A 15-minute ensemble average for the velocity measurements was used to reduce the standard error to approximately 0.6 cm s^{-1}. The ADCP measurements are confined in the upper 400-m water column. To obtain geostrophic currents, tidal currents were removed from the ADCP measurements by using a tidal current model for the Antarctic shelves, the details of which are provided in Padman *et al*. (2002). The geostrophic currents were computed from the thermal wind relation based on the *in-situ* density profile. For each CTD station, the measured current at the nearest ADCP station at 100 m was used as the reference velocity, and then the velocity shear was integrated upward or downward to obtain the geostrophic velocity at different depths. The reason to choose 100 m as the reference layer is that the wind-driven Ekman current can be neglected at this depth (Selph *et al.*, 2013), and thus the reference velocity is mostly geostrophic; meanwhile most of the ADCP measurements can reach the depth of 100 m. To explore the persistence of the slope currents in the study area over the long term, twenty-five years (1990–2014) of shipboard ADCP data from the Joint Archive for Shipboard ADCP Dataset (JASADCP, ftp:// ftp.soest.hawaii.edu/caldwell/adcp/INVNTORY/sou.html) covering the WAP region were used. Two cross-slope transects north of the SSIs (Fig.1c) were created to examine the cross-sectional profiles of the slope currents. The current value on each data point of the transects is the mean of current values from all of the JASADCP observations in 1990–2014 that fall in a bin enclosing this data point. The bin has the data point as the center, 40 km as the bin length (in the zonal direction) and 5–10 km as the bin width (in the meridional direction). There the current value on each data point is both a temporally and spatially averaged result.

In this study, labelling of the 2004 summer cruise transects starts with a letter 'S', and labelling of the 2006 winter cruise transects starts with a letter 'W' (Fig.1). The cross-slope transects designed were approximately perpendicular to the isobaths on the slope, and thus the cross-transect velocity is used to denote the along-isobath (or along-slope) velocity. A few transects, such as Transect S5 in the 2004 summer cruise, are composed of several sub-transects, and not all sub-transects are perpendicular to the isobaths. In this situation, only the sub-transects that are perpendicular to the isobaths were used to determine the cross-transect direction for the entire transect.

3 Results

Vertical distributions of potential temperature (θ), salinity (S), dissolved oxygen (DO), potential density (σ_θ), computed geostrophic currents, and the cross-transect ADCP current component along Transect S2 in the 2004 summer cruise are shown in Fig.2. The temperature profile displays a typical pattern of summertime water-mass distribution of Antarctic waters: a warm surface layer as the Antarctic Surface Water reaching approximately 2.5℃, the coldest layer at the depth of 100–200 m as the Antarctic Winter Water, and a warm layer below 200 m with the warm core centered about 400 m as the upper Circumpolar Deep Water (UCDW). One interesting feature is the existence of a cold ($-0.4℃ \le \theta \le 0.4℃$), fresh ($34.4\,g\,kg^{-1} \le S \le 34.6\,g\,kg^{-1}$) and oxygen-rich ($2.2\,mL\,L^{-1} \le DO \le 2.5\,mL\,L^{-1}$) water mass on the slope between 60.8°S and 60.85°S, which extends from the surface all the way to 1000 m, with two cold, fresh and oxygen-rich cores centered at 400 m and 550 m (Figs.2a–2c). The presence of this cold and fresh water mass creates a cross-slope density gradient with the isopycnals shoaling toward the coast south of 60.83°S (Fig.2d). The ADCP measurement shows that the area north of 60.83°S is dominated by the strong northeastward Antarctic Circumpolar Current (ACC) from surface to 400 m, while in the area south of 60.83°S, the northeastward current in the upper layer turns to southwestward below 200 m (Fig.2f). ADCP transects S1 and S3 are located in a similar area. The measured cross-transect currents on S1 and S3 are shown in Fig.3. Southwestward currents are prominent over the upper slope north of the EI on both of the two transects, and the velocity reaches approximately 20 cm s^{-1} and 30 cm s^{-1} on S1 and S3, respectively.

During the 2006 winter cruise, Transect W1 also crosses the STR, SG and extends to the slope of the EI (Fig.1c), and this allows us to examine the seasonal variation of the slope currents in this area. The vertical profiles of potential temperature, salinity, dissolved oxygen, potential density, computed geostrophic currents, and cross-transect ADCP current component on Transect W1 are shown in Fig.4. North of 60.75°S, the upper 200 m of the water column is occupied by the cold and fresh Antarctic Surface Water (Figs.4a and b), while the water column below 200 m is occupied by UCDW. South of 60.75°S, a cold ($-0.5℃ \le \theta \le 0.3℃$), fresh ($34.3\,g\,kg^{-1} \le S \le 34.6\,g\,kg^{-1}$) and oxygen-rich ($1.8\,mL\,L^{-1} \le DO \le 2.2$ mL L^{-1}, Fig.4c) water with similar characteristics to

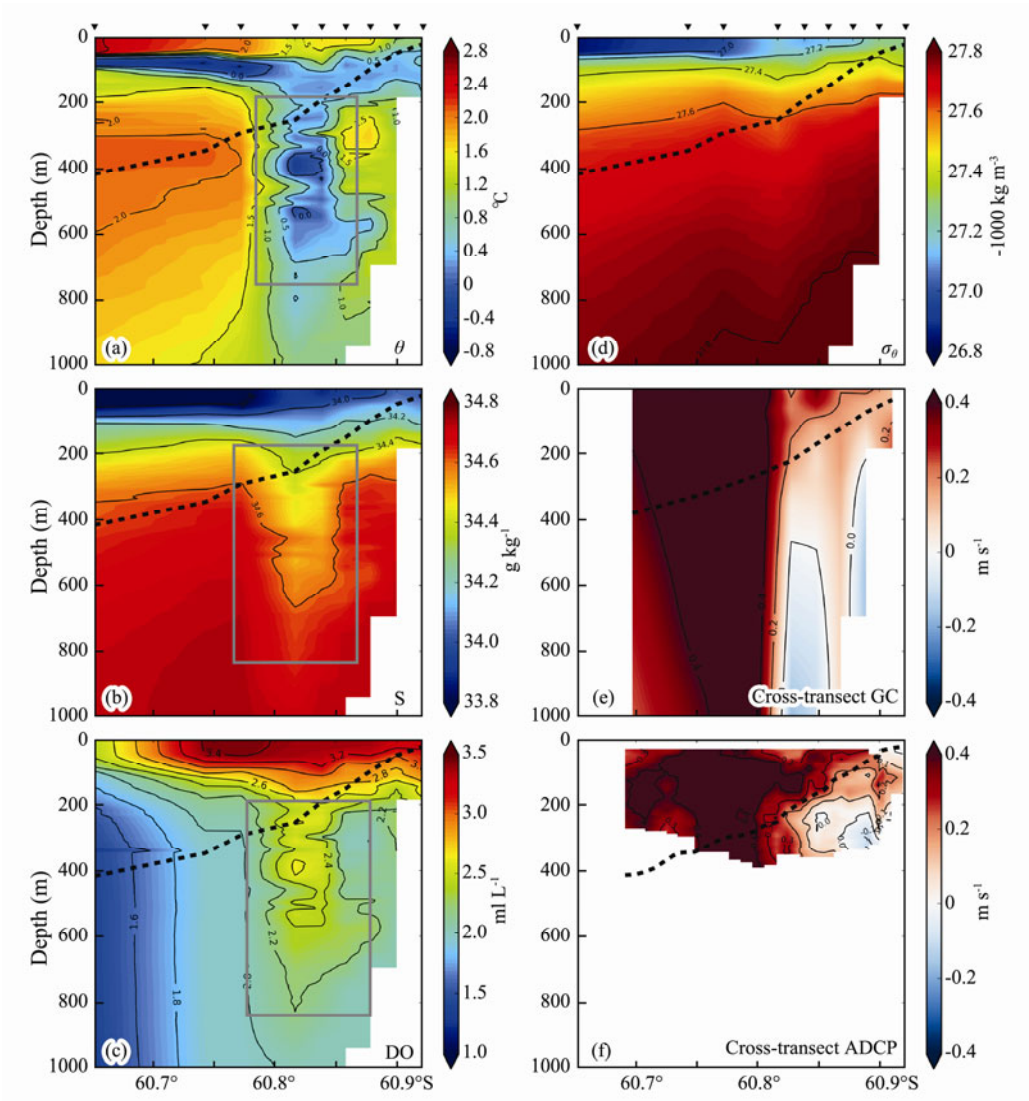

Fig.2 Vertical profiles of (a) potential temperature, (b) salinity, (c) dissolved oxygen, (d) potential density, (e) calculated geostrophic current, and (f) cross-transect current from the ADCP measurement along Transect S2 from the 2004 summer cruise. See Fig.1b for the transect locations. The dashed, black line indicates the bathymetry, and the depth value (m) on this line is the bottom depth divided by 10. The black triangles mark the locations of the CTD stations. The grey boxes in (a), (b) and (c) label the cold ($-0.4℃ \le \theta \le 0.4℃$), fresh ($34.4\,g\,kg^{-1} \le S \le 34.6\,g\,kg^{-1}$) and oxygen-rich ($2.2\,mL\,L^{-1} \le DO \le 2.5\,mL\,L^{-1}$) water mass found on this transect. Red (blue) color in (e) and (f) indicates eastward (westward) current.

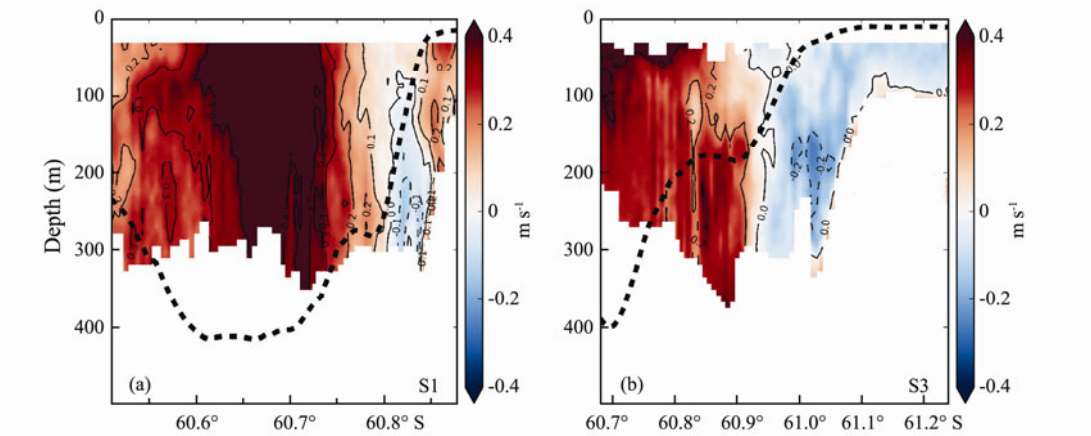

Fig.3 Vertical profiles of the cross-transect current from the ADCP measurements along Transect (a) S1 and (b) S3 from the 2004 summer cruise. See Fig.1b for the transect locations. The dashed, black line indicates the bathymetry, and the depth value (m) on this line is the bottom depth divided by 10. Red (blue) color indicates eastward (westward) current.

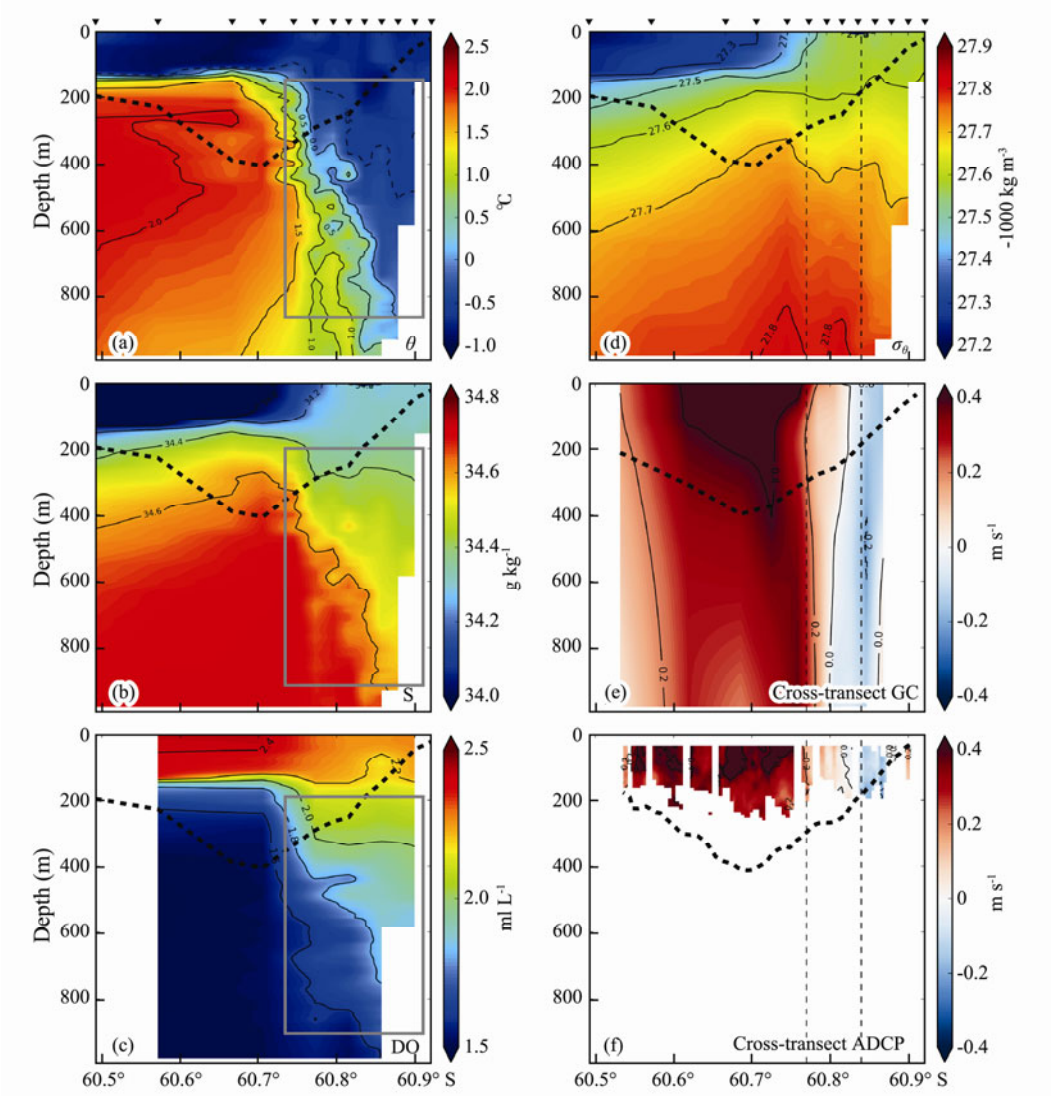

Fig.4 Vertical profiles of (a) potential temperature, (b) salinity, (c) dissolved oxygen, (d) potential density, (e) calculated geostrophic current, and (f) cross-transect current from the ADCP measurement along Transect W1 from the 2006 austral winter cruise. See Fig.1c for the transect location. The dashed, black line indicates the bathymetry, and the depth value (m) on this line is the bottom depth divided by 10. The black triangles mark the locations of the CTD stations. The grey boxes label the cold ($-0.5℃ \leq \theta \leq 0.3℃$), fresh ($34.3\,g\,kg^{-1} \leq S \leq 34.6\,g\,kg^{-1}$) and oxygen-rich ($1.8\,mL\,L^{-1} \leq DO \leq 2.2\,mL\,L^{-1}$)) water mass found on this transect. The thin dashed lines in (d), (e) and (f) show the center locations of the isopycnal-tilting sections mentioned in the text. Red (blue) color in (e) and (f) indicates eastward (westward) current.

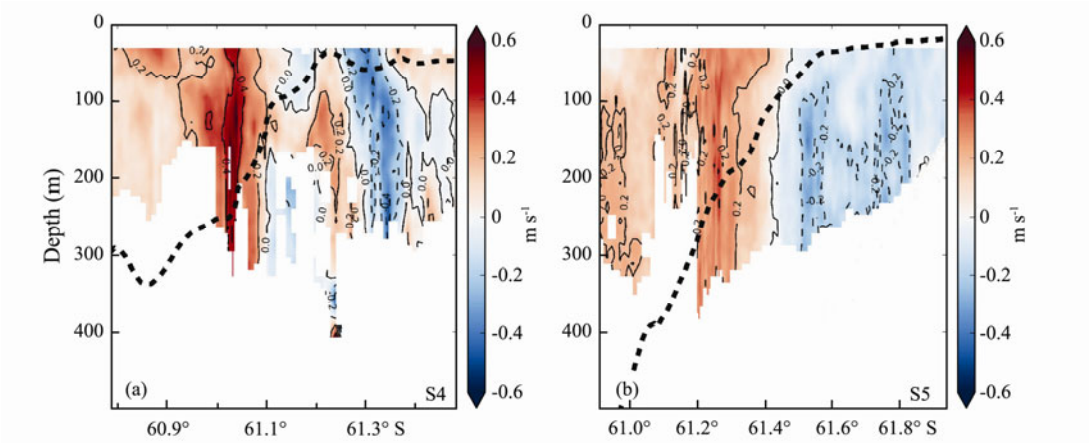

Fig.5 Vertical profiles of cross-transect currents from ADCP measurements along Transect (a) S4 and (b) S5 from the 2004 austral summer cruise. See Fig.1b for the transect locations. The dashed, black line indicates the bathymetry, and the depth value (m) on this line is the bottom depth divided by 10. Red (blue) color indicates eastward (westward) current.

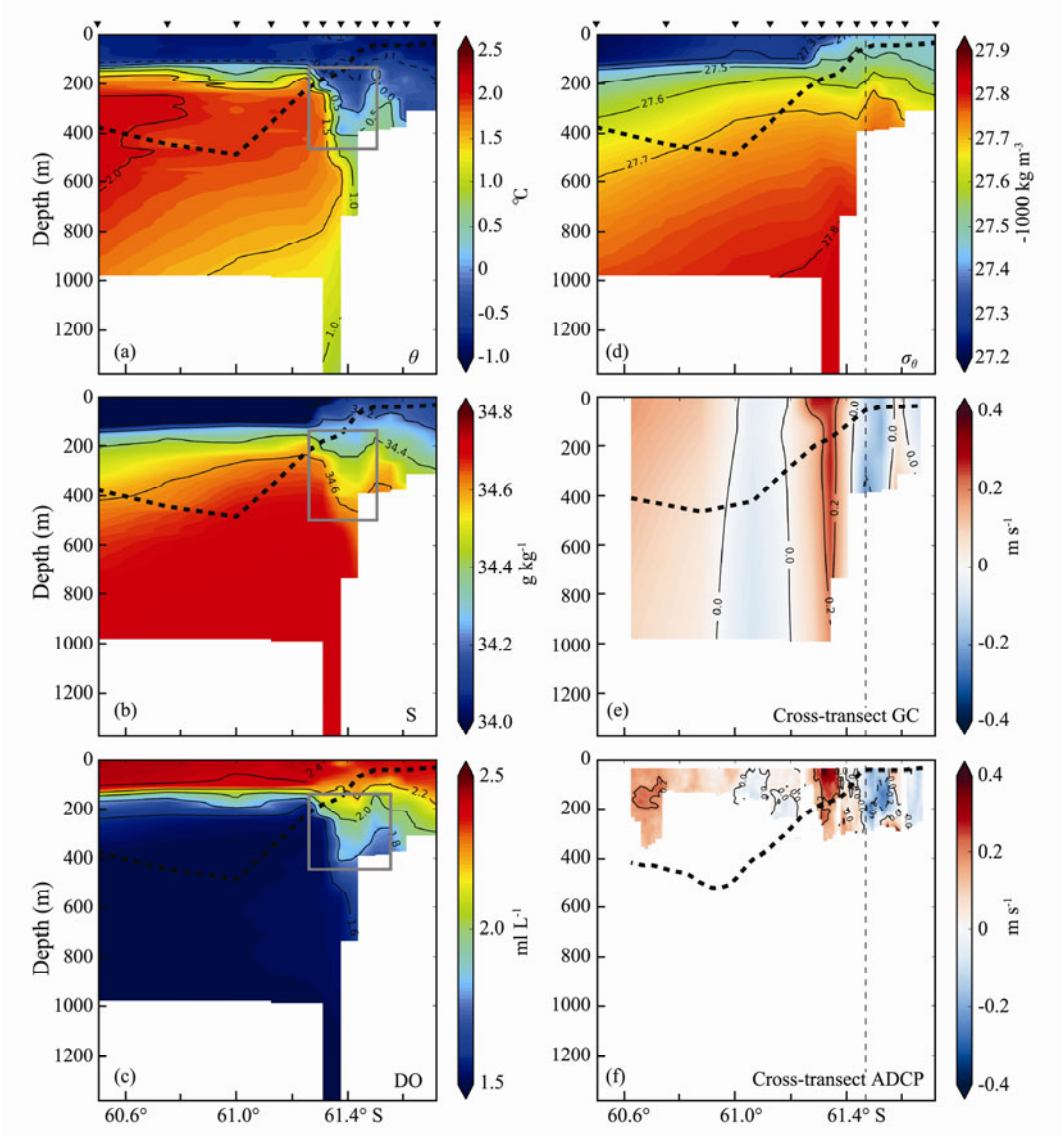

Fig.6 Vertical profiles of (a) potential temperature, (b) salinity, (c) dissolved oxygen, (d) potential density, (e) calculated geostrophic current, and (f) cross-transect current from the ADCP measurement along Transect W2 from the 2006 winter cruise. See Fig.1c for the transect location. The dashed, black line indicates the bathymetry, and the depth value (m) on this line is the bottom depth divided by 10. The black triangles mark the locations of the CTD stations. The grey boxes in (a), (b) and (c) label the cold ($-0.5℃ \le \theta \le 0.5℃$), fresh ($34.4\,g\,kg^{-1} \le S \le 34.5\,g\,kg^{-1}$) and oxygen-rich ($1.9\,mL\,L^{-1} \le DO \le 2.1\,mL\,L^{-1}$) water mass found on this transect. The thin dashed lines in (d), (e) and (f) show the center locations of the isopycnal-tilting sections mentioned in the text. Red (blue) color in (e) and (f) indicates eastward (westward) current.

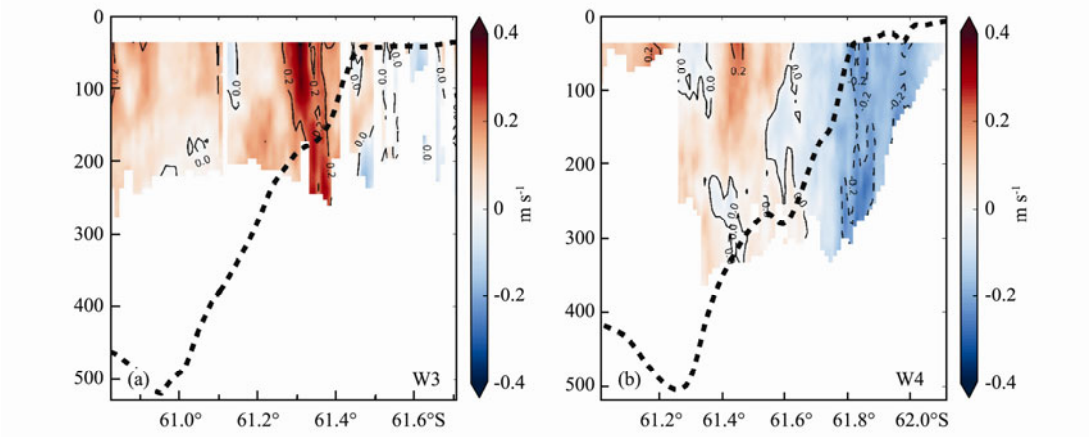

Fig.7 Vertical profiles of cross-transect currents along Transect (a) W3 and (b) W4 from the 2006 austral winter cruise. See Fig.1c for the transect locations. The dashed, black line indicates the bathymetry, and the depth value (m) on this line is the bottom depth divided by 10. Red (blue) color indicates eastward (westward) current.

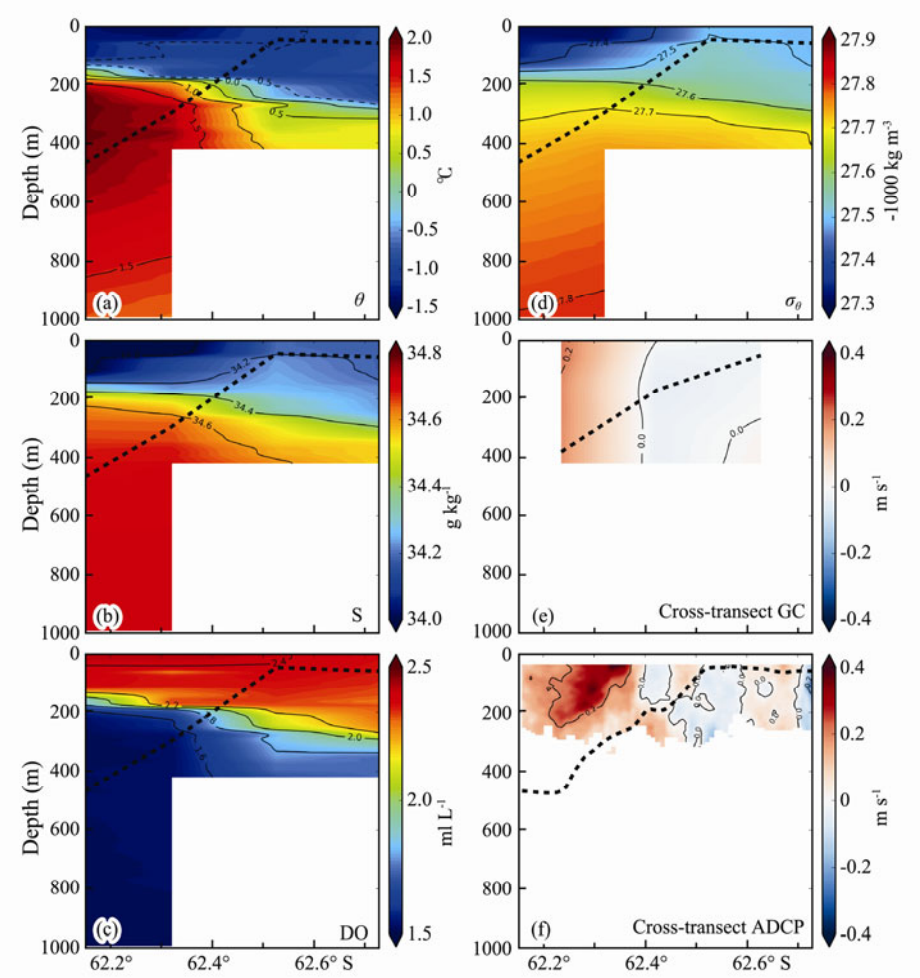

Fig.8 Vertical profiles of (a) potential temperature, (b) salinity, (c) dissolved oxygen, (d) potential density, (e) calculated geostrophic current, and (f) cross-transect current from the ADCP measurement along Transect W5 from the 2006 winter cruise. See Fig.1c for the transect locations. The dashed, black line indicates the bathymetry, and the depth value (m) on this line is the bottom depth divided by 10. The black triangles mark the locations of the CTD stations. Red (blue) color in (e) and (f) indicates eastward (westward) current.

the one found on Transect S1 in 2004 summer (Figs.2a–c) extends from 200 m to below 800 m. Water in the upper 200 m of this region is saltier and poorer in oxygen than surrounding waters. In Fig.4f, a strong northeastward current is observed over the lower slope, which reaches approximately 50 cm s^{-1}. Meanwhile, over the upper slope (60.82°S–60.88°S), a southwestward current is observed in the depth range of 0–200 m, with a magnitude lower than 20 cm s^{-1}.

Along the continental slope west of the EI and north of the SSIs, continual southwestward slope currents are observed. Vertical profiles of cross-transect currents from the ADCP measurements along Transect S4 and S5 in the 2004 summer cruise (Fig.5), which are located between the EI and the King George Island (Fig.1b), both show southwestward currents over the upper slope. On Transect S4, which is closer to the EI, the westward slope currents present between 61.1°S and 61.2°S are discontinuous in the vertical direction. On Transect S5, the westward currents over the upper slope increase from 10 cm s^{-1} at surface to 30 cm s^{-1} below 100 m.

During the 2006 winter cruise, four cross-slope transects – W2, W3, W4 and W5, are located north of the SSIs (Fig.1c). Current patterns on these transects are shown in Fig.6, Fig.7 and Fig.8. Vertical profiles of the hydrographic variables and currents along Transect W2 are shown in Fig.6. Similar to Transect W1, a cold (−0.5 ℃≤ $\theta \leq$ 0.5℃), fresh (34.4 g kg^{-1} ≤ $S \leq$ 34.5 g kg^{-1}) and oxygen-rich (1.9 mL L^{-1} ≤ DO ≤ 2.1 mL L^{-1}) water mass is present on the outer shelf and the upper slope of the SSIs (61.22°S–61.5°S), extending from surface to the depth of about 400 m (Figs.6a–6c). Below 300 m, the water is a mixture of the warm UCDW and the cold and fresh water on the upper slope.

On Transect W3 (Fig.7a), westward currents are not obvious, which is probably due to the fact that the ADCP measurements are confined in the upper 200 m of the water column and the current reversal has been weak until this depth. Westward currents appear again on Transect W4 on the upper slope with a nearly barotropic structure (Fig.7b), and there is a slight intensification of the westward currents below 150 m near the outer shelf and upper slope (61.8°S–61.9°S). Transect W5 is located near the Boyd Strait, *i.e.*, the western end of the SSIs. Signature of the cold, fresh and oxygen-rich water mass can still be identified on the upper slope and the outer shelf (Fig.

8a–c), though much weaker (−0.5℃ ≤ θ ≤ 1.2℃ and 1.7 mL L^{-1} ≤ DO ≤ 2.2 mL L^{-1}) compared to those on transects in the east (such as Transect W1 and W2). Southwestward currents occur near the shelf break (62.45˚S–62.6˚S) in the ADCP measurements (Fig.8f) and are slightly intensified below 250 m.

4 Discussion

4.1 Horizontal Circulation Field

To better show the spatial variation of slope currents in the WAP area, as well as the relation of the slope currents to the atmospheric forcing, maps of surface wind and currents at different depth levels for the 2004 and 2006 cruises are displayed in Fig.9 and Fig.10, respectively. From Fig.9, surface (31 m) currents (Fig.9b) over the slope of the SSIs and the SG are eastward, which are affected by the eastward ACC over the lower slope and the westerly wind over the upper slope. At 250 m (Fig.9c), southwestward currents are observed over the upper slope in the SG and north of the SSIs. In 2006 (Fig.10), westward currents over the upper slope are observed at both

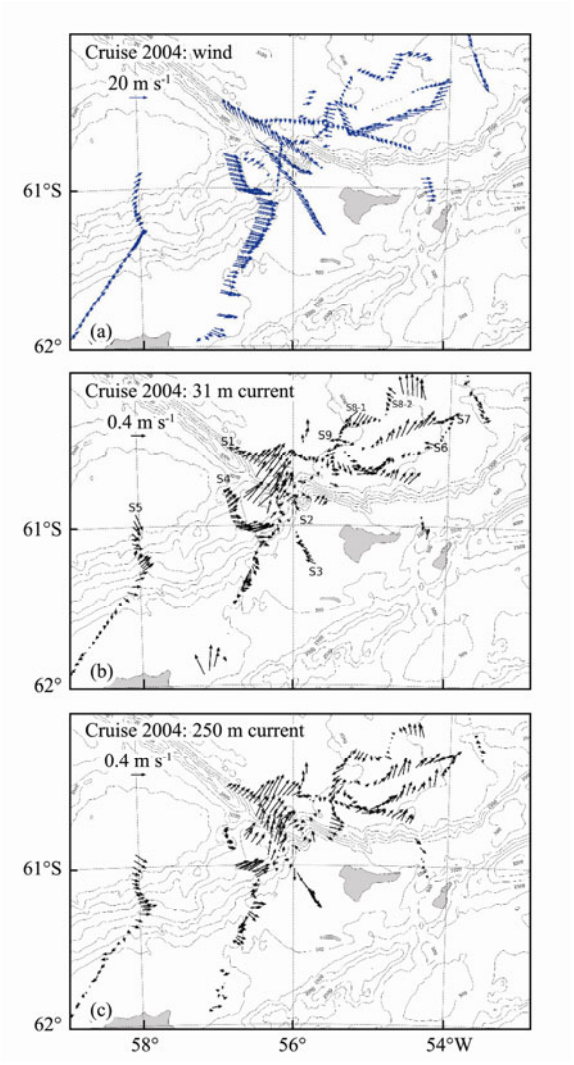

Fig.9 Maps of observed (a) surface winds, (b) currents at 31 m and (c) currents at 250 m from the 2004 summer cruise. Depth contours shown (in m) are 0–4000 m by 500-m increments.

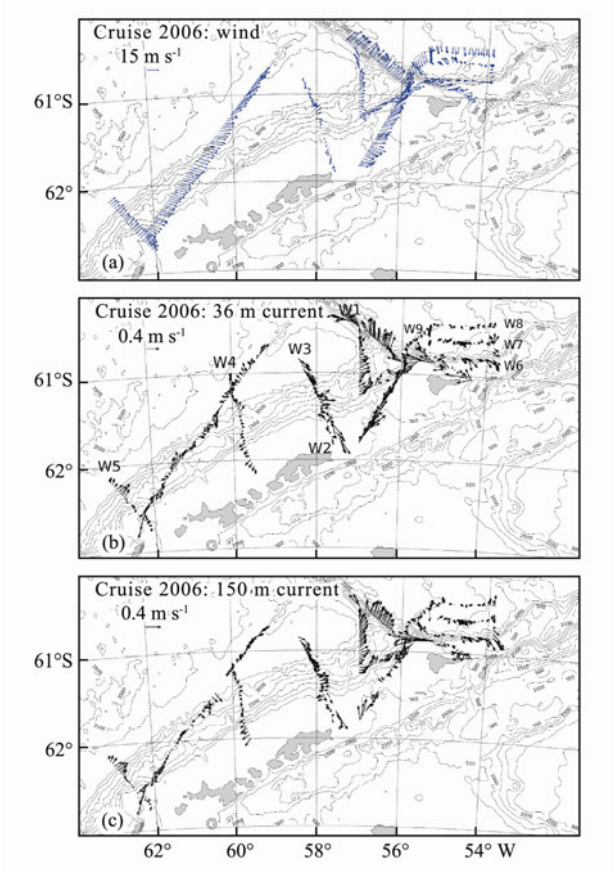

Fig.10 Maps of observed (a) surface winds, (b) currents at 36 m and (c) currents at 150 m from the 2006 winter cruise. Depth contours shown (in m) are 0–4000 m by 500-m increments.

surface (36 m, Fig.10b) and 150 m (Fig.10c). The westward currents at surface seem not driven by wind, since wind over this region is eastward (Fig.10a), and the currents are probably associated with eddy processes near the southern ACC front generated by baroclinic instability. It is noted that in both 2004 and 2006, southwestward currents are observed on the transects east of the SG, including Transect S8-1 and S9 in 2004 and Transect W9 in 2006 and both in surface and deeper layers. These southwestward currents could be strongly affected by the dynamics of ACC passing through the SG that interacts with the northern slope of the EI (Zhou *et al.*, 2013). Southwestward currents on these transects are stronger at 150/250 m (20–40 cm s^{-1}) than at surface (about 10 cm s^{-1}), and could play a role in carrying water from the Scotia Sea, which probably comes from the slope area of the Weddell Sea, into the SG, as will be discussed in Section 4.3.

4.2 Dynamical Balance of the Slope Currents

4.2.1 Slope currents near the SG

In Fig.2, a cold (−0.4℃ ≤ θ ≤ 0.4℃), fresh (34.4 g kg^{-1} ≤ S ≤ 34.6 g kg^{-1}) and oxygen-rich (2.2 mL L^{-1} ≤ DO ≤ 2.5 mL L^{-1}) water mass is observed over the upper slope north of the EI (Figs.2a–c). The existence of this special water mass results in a minimum value of potential den-

sity at around 60.83°S on Transect S2 (Fig.2d), as the effect of lower salinity on density weighs out that of lower temperature. South of 60.83°S, currents in the surface layer are affected by the westerly wind (Fig.9a) and flow northeastward. However, below 200 m, shoaling of the isopycnals toward the south, which is due to the presence of the cold and fresh water mass, results in a negative offshore density gradient ($d\rho/dy < 0$), and then in a positive vertical shear of the cross-transect velocity ($du/dz > 0$) according to the thermal wind balance. Such vertical shear is associated with a reversal of the northeastward current at surface to southwestward current below 200 m (Figs.2e and f). It can be seen that near the shelf break (south of 60.87°S), within the depth range covered by observations (0–400 m), the southwestward slope currents in Fig.2e (the computed geostrophic current) and 2f occur at similar depths (below 200 m) and have similar magnitudes of 10 cm s^{-1}, indicating that the geostrophic current can well explain the observed slope current. North of 60.83°S, the strong eastward current (Fig.2f) is considered to be the southern boundary of the ACC that is steered to the south by the STR and crosses the narrow SG between the EI and STR in the form of a jet (Zhou *et al*., 2013). Since the horizontal density gradient (and thus the vertical shear of the along-slope velocity) is small in this region, the computed geostrophic current basically resembles the measured current, which is characterized by a strong, eastward current at nearly all depths (Fig.2e).

It is noted that on Transect S1 (Fig.3a), westward slope currents occur below the surface layer, similar to the situation on Transect S2. There are no CTD measurements on this transect, precluding the analysis of geostrophic balance. We infer that the reversal of the cross-transect current from eastward at surface to westward in deep water is caused by the horizontal density gradient associated with the water mass distribution, as on Transect S2. On Transect S3 (Fig.3b), the westward current extends all the way from surface to deep layers. The surface current is in the opposite direction to the wind shown in Fig.9a, so the westward current could be driven by eddies near the boundary of the southern ACC. The reason of the depth-intensified southwestward current below 150 m may be the same as that for Transect S2 and S1.

Similar to the 2004 summer cruise, a cold ($-0.5℃ \le \theta \le 0.3℃$), fresh ($34.3\,g\,kg^{-1} \le S \le 34.6\,g\,kg^{-1}$) water mass was found on Transect W1 of the 2006 winter cruise (Fig. 4), which is located in the slope area of the SG south of 60.75°S. The presence of this water mass results in a positive offshore density gradient between 60.75°S and 60.8°S (Fig.4d), which then leads to an intensification of the eastward current below 200 m (Fig.4e). However, intrusion of the warm and salty UCDW into the cold and fresh water mass, which occurs between 60.8°S and 60.86°S, causes a slight shoaling of the isopycnals towards the south. This results in a positive vertical shear of the cross-transect velocity in this region, and thus the westward current at surface are slightly intensified below 200 m. From Fig.4d, such intrusion mainly occurs below 200 m, and therefore above 200 m the measured current and the geostrophic current on Transect W1 both display a barotropic structure with similar magnitudes.

4.2.2 Slope currents north of the SSIs

On Transect W2 of the 2006 winter cruise (Fig.6), an upwelling of warm, salty and low-oxygen water mass exists on the upper slope between 61.4°S and 61.6°S, which should be associated with the intrusion of UCDW towards the shelf due to eddy processes, topographic steering or upwelling (Moffat *et al.*, 2009; Stewart and Thompson, 2015, 2016). Such intrusion causes shoaling of the isopycnals toward the south between 61.4°S and 61.6°S, resulting in an intensification of the westward currents below 200 m in the profile of geostrophic current (Fig.6e). Such intensification is also observed in the ADCP measurement (Fig.6f). In both Figs.6e and 6f, westward currents are present between 60.9°S and 61.2°S. Currents in this region are quite weak at surface due to the weak cross-transect component of wind (Fig.10a). Below 200 m, the slight southward shoaling of isopynals associated with the upwelling of UCDW results in a weak vertical shear of the cross-transect velocity, inducing weak westward currents. The computed geostrophic current pattern is in good agreement with the observed current pattern. On Transect W5, the isopycnal tilting is much weaker compared to those on the other transects in the 2006 cruise (Fig.8d), possibly because of the low resolution of the hydrography observations on this transect and thus the missing details in the isopycnal structure. As a result, the geostrophic current is almost barotropic (Fig.8e). However, an intensification of southwestward currents can be identified near the shelf break below 200 m between 62.45°S and 62.6°S (Fig.8f), and such feature could be associated with the onshore intrusion of UCDW as revealed in the low-resolution θ (Fig.8a) and DO (Fig. 8c) patterns.

4.2.3 Long-term mean slope currents derived from the JASADCP data

In both of the 2004 summer and 2006 winter cruises, southwestward slope currents are found to be present on the upper slope of the SSIs and EI (Figs.2–8). However, it is known that the ASC would fluctuate at a range of time scales. To investigate if the southwestward slope currents are a persistent feature over the long term, current measurements from the JASADCP dataset covering the WAP region spanning the period 1990–2014 were analyzed. Long-term mean currents on the created cross-slope transects north of the SSIs, which are derived by the method described in Section 2, were examined separately for the austral spring (September to November, SON), summer (December to February, DJF), autumn (March to May, MAM) and winter (June to August, JJA) seasons. It is noted that on Transect JS1 (Fig.11), southwestward slope currents occur on the upper slope in all seasons. The southwestward currents in summer and winter are approximately 20 cm s^{-1}, which are stronger than the spring

and fall values that are about 10 cm s^{-1}. Meanwhile, the southwestward slope currents are slightly depth-intensified below 100 m in summer and winter (Figs.11b and d). Similar to Transect JS1, southwestward slope currents are present on the upper slope of the SSIs on JS2 (Fig.12), with magnitudes lower than 20 cm s^{-1}. Currents on the lower slope are mainly affected by ACC and flow northeastward. These results demonstrate that the southwestward slope currents in our study area are a persistent feature over time.

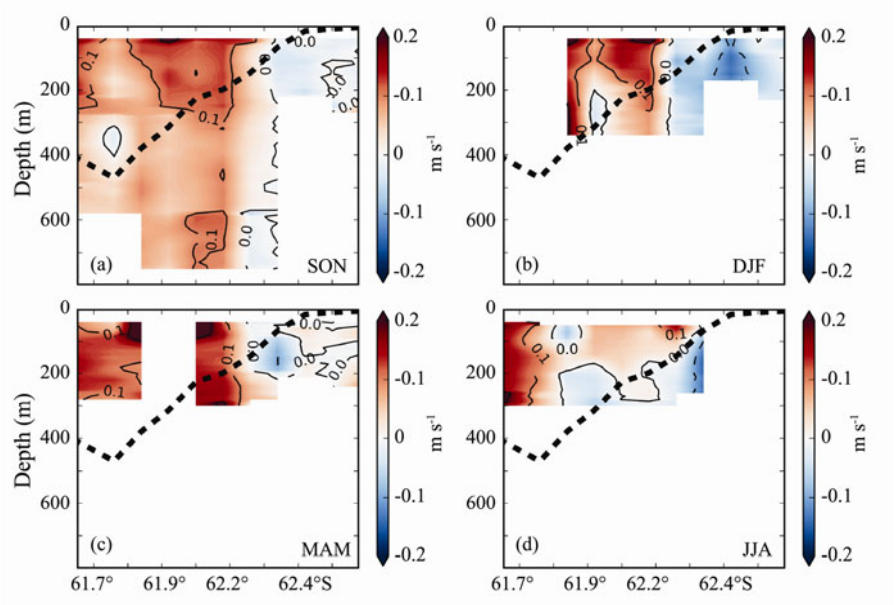

Fig.11 Vertical profiles of cross-transect currents along Transect JS1 based on JASADCP datasets in austral (a) spring, (b) summer, (c) fall and (d) winter. See Fig.1c for the transect location. The dashed, black line indicates the bathymetry, and the depth value (m) on this line is the bottom depth divided by 10. Red (blue) color indicates eastward (westward) current.

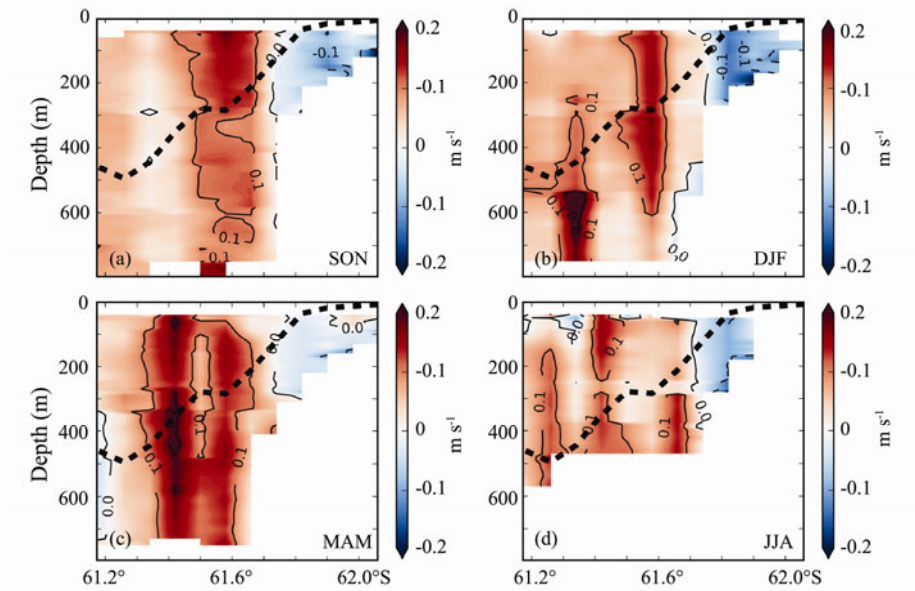

Fig.12 Vertical profiles of cross-transect currents along Transect JS2 based on the JASADCP data in austral (a) spring, (b) summer, (c) fall and (d) winter. See Fig.1c for the transect location. The dashed, black line indicates the bathymetry, and the depth value (m) on this line is the bottom depth divided by 10. Red (blue) color indicates eastward (westward) current.

4.3 Origin of the Cold and Fresh Water Masses

Cold, fresh and oxygen-rich water masses have been found on the transects with CTD observations in the SG and north of the SSIs both in the 2004 summer and the 2006 winter cruises, which are quite distinct from the surrounding warm, salty and low-oxygen UCDW below 200 m. From the analyses in Section 4.2, the westward slope currents are directly or indirectly influenced by the presence of these cold and fresh water masses, so it is interesting to know where this water comes from. Water masses near the SG have four sources: shelf water north of the SSIs and the EI, the Bransfield Strait water (BSW), the ACC water, and the Weddell Sea Deep water (WSDW) (Zhou *et al.*, 2010; Frants *et al.*, 2013). These water masses are labeled in the potential-temperature-salinity (θ-S) diagram in Fig.14a. WSDW originates from the Circumpolar Deep Water (CDW), and contributions from

sea ice formation processes have made it significantly cooler and saltier than the shelf waters from the SSIs and EI (Zhou *et al.*, 2013). BSW originates from the Weddell Sea, and their θ-S characteristics are significantly modified by local processes (Gordon *et al.*, 2000; Nowlin and Klinck, 1986; Orsi *et al.*, 1995; Ross *et al.*, 2013). Six transects with CTD measurements from the 2006 cruise – CB, CS, CN, W1, W2 and W5 were analyzed to investigate the source of the cold ($-0.5℃ \le \theta \le 0.5℃$), fresh ($34.4\,g\,kg^{-1} \le S \le 34.6\,g\,kg^{-1}$) and oxygen-rich ($1.8\,mL\,L^{-1} \le DO \le 2.2\,mL\,L^{-1}$) water mass on the upper slope of the SG. Locations of these transects and the specific stations used for the water-mass analysis are shown in Fig.13. The θ-S and potential-temperature-dissolved-oxygen (θ-DO) diagrams for waters on these transects are displayed in Fig.14. From the θ-S diagram (Fig.14b), below 1000 m ($\sigma_\theta > 27.8\,kg\,m^{-3}$), the water characteristics at Sta. 59, which is on the transect on the southern slope of the Scotia Sea, shows similarity to that at Sta. 94 located on the slope of the Weddell Sea. This suggests a connection between the deep waters on the slope of the Weddell Sea and the southern slope of the Scotia Sea. As mentioned

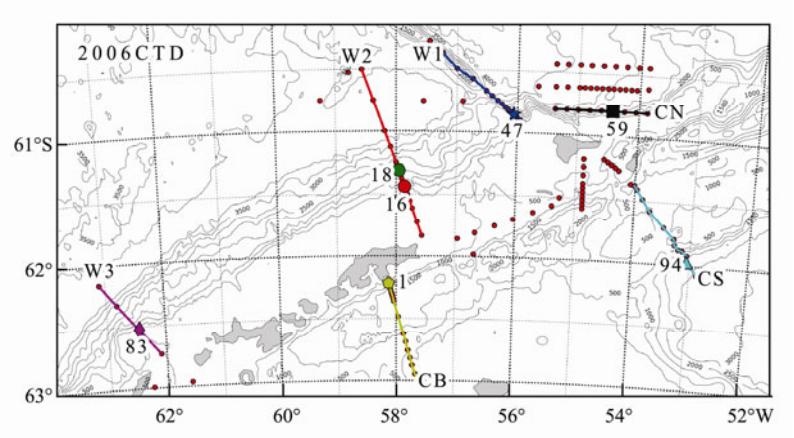

Fig.13 CTD stations (dots) and transects (lines) from the 2006 winter cruise. The yellow, cyan, black, blue, red and magenta lines mark Transect CB, CS, CN, W1, W2 and W5, respectively. Station 1, 94, 59, 47, 16, 18 and 83 are used in the water mass analysis in Fig.14. Depth contours shown (m) are 0–4000 m by 500-m increments.

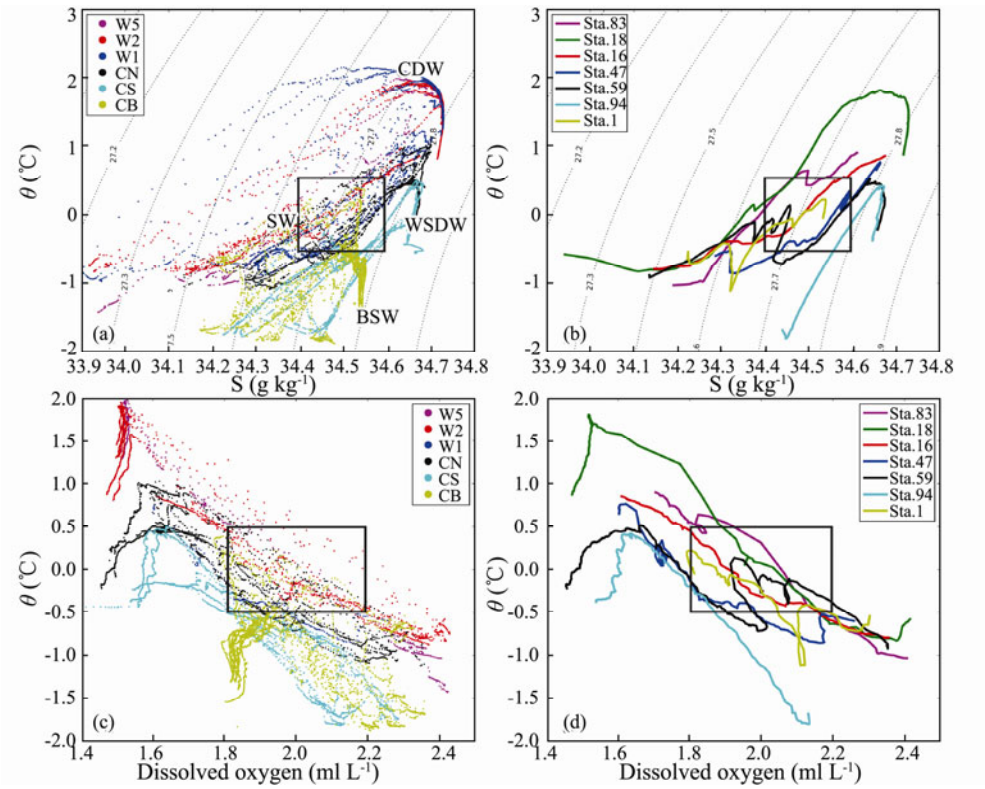

Fig.14 (a and b) potential-temperature-salinity (θ-S) and (c and d) potential-temperature-dissolved oxygen (θ-DO) diagrams for transects (a and c) and stations (b and d) shown in Fig.13. The yellow, cyan, black, blue, red and magenta dots are the θ-S pairs and θ-DO pairs on Transect CB, CS, CN, W1, W2 and W5, respectively. The black boxes in (a), (b), (c) and (d) mark the range of the cold, fresh and oxygen-rich water masses found in the upper slope and shelf region north of the SSIs and EI. The abbreviations are the Circumpolar Deep water (CDW), the Shelf Water (SW), the Bransfield Strait Water (BSW) and the Weddell Sea Deep Water (WSDW).

before, Nowlin and Zenk (1988) found that WSDW would enter the Scotia Sea through deep gaps in the Scotia Island Arc and may flow southwestward into the Drake Passage through the SG (Naveira Garabato *et al.*, 2002; Youngs *et al.*, 2015). Since observations at Sta. 47 are confined in the upper 1000 m, it is hard to tell if the deep waters from Sta. 94 can be further carried westward through the SG and reach Sta. 47. In the section where the cold, fresh and oxygen-rich water mass lies in Fig. 14b (marked by the black box), Sta. 47 and 59 show similar water characteristics in both the θ–S and θ–DO diagrams, suggesting that the cold and fresh water mass in the SG originates from the southern shelf and slope area of the Scotia Sea. In this section, the water characteristics at Sta. 47 and 59 demonstrate some similarity to those at Sta. 94, while overall water at the former two stations are warmer and saltier. This feature was also found in Shi *et al.* (2016). The water masses at Sta. 59 and 47 could be a result of mixing between WSDW and CDW.

Sta. 18 is close to Sta. 16 geographically, and they are on the same cross-slope transect, but the water characteristics at Sta. 18 are obviously different from that at Sta. 16 in deep water. Deep water at Sta. 18 is from the UCDW (Fig.14a). It has been known that cold BSW, either originating from the Weddell Sea or from local production, could turn around at the northern end of the SSIs and then move southward by currents occupying the inner SSIs shelf (Ardelan *et al.*, 2010; Jiang *et al.*, 2013; Thompson *et al.*, 2009), so BSW could have a considerable effect on water properties over the shelf and slope north of the SSIs. In the section where the cold and fresh water lies in the θ–S and θ–DO diagrams in Fig.14, water characteristics at Sta. 16 ($\sigma_\theta > 27.8\,\mathrm{kg\,m^{-3}}$) are quite similar to those at Sta. 1, which is located on the northern slope of the Bransfield Strait. This indicates that BSW could be the source of the cold and fresh water on the shelf and upper slope north of the SSIs.

Comparing the water properties on Transect W1 (Fig. 4), W2 (Fig.6) and W5 (Fig.8) from the 2006 cruise, or at Sta. 47, Sta. 16 and Sta. 83 on these transects, we can see that below 200 m, the cold and fresh water mass becomes warmer and saltier as it goes westward, which is a result of mixing with the warm UCDW. In the upper 200 m, Sta. 83, Sta.16, Sta. 18, Sta. 47 and Sta. 1 display the same water characteristics of the Antarctic Surface Water in austral winter (Fig.14b).

5 Conclusions

Hydrography and velocity data were analyzed for eighteen transects in the area north of the EI and the SSIs during an austral summer cruise in 2004 and a winter cruise in 2006, to reveal the patterns and dynamical balance of the slope currents in this region. Southwestward currents are found to be present over the upper slope near the shelf break in the SG, westward all the way to the slope area north of the SSIs, with magnitudes of 10–30 cm s^{-1}. Cross-transect (along-slope) current analysis based on 25 years of shipboard ADCP measurements in the WAP region demonstrates the persistence of the southwestward slope currents over the long term. Near the SG, vertical shear of the deep slope currents is in thermal wind balance with the cross-slope density gradient, which is created by the presence of a water mass colder, fresher and oxygen-richer than ambient waters. Results from water mass analysis suggest that this cold and fresh water originates from the southern shelf and slope area of the Scotia Sea, which could have its ultimate source on the Weddell Sea slope. The cold and fresh water on the outer shelf and upper slope north of the SSIs originates majorly from the Bransfield Strait. North of the SSIs, vertical structure of the southwest, deep slope currents near the shelf break is associated with the horizontal density gradient created by the intrusion of UCDW onto the shelf.

This study has identified the southwestward slope currents in the WAP, which indicates that the ASC is continued after it turns around the Antarctic Peninsula (Heywood *et al.*, 2004), though with lower magnitudes. In this study, the hydrographic measurements used are confined in the upper 1000-m water column, while the shipboard ADCP measurements are only confined in the upper 400-m water column. The slope current features revealed can be useful for studies of biomass transport in the WAP region in the upper ocean, such as the transport of krill larvae, which mainly stay in the upper 1000-m water column. However, with the limited depth of observations, structures of the slope currents over the full water column cannot be revealed, and the total volume transports by these currents cannot be evaluated, which are the limitations of this study. Also, more work should be done to explore the ultimate forcing mechanisms of the slope currents and the processes controlling their dynamical balances, such as the transport of the cold and fresh water from its source region into the WAP, and characteristics of the onshore CDW intrusion. These processes can be examined using a high-resolution ocean circulation model, which will be the future work of this study.

Acknowledgements

This work was funded by the National Natural Science Foundation of China (No. 41406006). Y. Z was sponsored by Shanghai Sailling Program (No. 15FY1406400). We would like to acknowledge the hard work by crews of the A.S.R.V.L.M. Gould and R.V.I.B.N.B. Palmer cruises. We would also like to acknowledge the anonymous reviewers for improving the quality of this manuscript.

References

Ardelan, M. V., Holmhansen, O., Hewes, C. D., Reiss, C. S., Silva, N. S., Dulaiova, H., Steinnes, E., and Sakshaug, E., 2010. Natural iron enrichment around the Antarctic Peninsula in the Southern Ocean. *Biogeosciences*, **7** (1): 11-25.

Capella, J. E., Ross, R. M., Quetin, L. B., and Hofmann, E. E., 1992. A note on the thermal structure of the upper ocean in the Bransfield Strait-South Shetland Islands region. *Deep Sea Research Part A. Oceanographic Research Papers*, **39** (7-8):

1221-1229, DOI: 10.1016/0198-0149(92)90065-2.

Dong, S., Sprintall, J., Gille, S. T., and Talley, L., 2008. Southern Ocean mixed-layer depth from Argo float profiles. *Journal of Geophysical Research*, **113** (C6), DOI: 10.1029/2006JC004051.

Flexas, M. M., Schodlok, M. P., Padman, L., Menemenlis, D., and Orsi, A. H., 2015. Role of tides on the formation of the Antarctic Slope Front at the Weddell-Scotia Confluence. *Journal of Geophysical Research: Oceans*, **120** (5): 3658-3680, DOI: 10.1002/2014JC010372.

Frants, M., Gille, S. T., Hewes, C. D., Holm-Hansen, O., Kahru, M., Lombrozo, A., Measures, C. I., Greg Mitchell, B., Wang, H., and Zhou, M., 2013. Optimal multiparameter analysis of source water distributions in the Southern Drake Passage. *Deep Sea Research Part II: Topical Studies in Oceanography*, **90**: 31-42, DOI: 10.1016/j.dsr2.2012.06.002.

Gordon, A. L., Mensch, M., Zhaoqian, D., Smethie, W. M., and Bettencourt, J., 2000. Deep and bottom water of the Bransfield Strait eastern and central basins. *Journal of Geophysical Research*, **105** (C5): 11337-11346.

Heywood, K. J., Naveira Garabato, A. C., Stevens, D. P., and Muench, R. D., 2004. On the fate of the Antarctic Slope Front and the origin of the Weddell Front. *Journal of Geophysical Research: Oceans*, **109**: C06021.

Heywood, K. J., Schmidtko, S., Heuzé, C., Kaiser, J., Jickells, T. D., Queste, B. Y., Stevens, D. P., Wadley, M., Thompson, A. F., and Fielding, S., 2014. Ocean processes at the Antarctic continental slope. *Philosophical Transactions of the Royal Society of London A: Mathematical, Physical and Engineering Sciences*, **372** (2019): 20130047.

Jiang, M., Charette, M. A., Measures, C. I., Zhu, Y., and Zhou, M., 2013. Seasonal cycle of circulation in the Antarctic Peninsula and the off-shelf transport of shelf waters into southern Drake Passage and Scotia Sea. *Deep Sea Research Part II Topical Studies in Oceanography*, **90** (6): 15-30.

Locarnini, R. A., Whitworth, T., and Nowlin, W. D., 1993. The importance of the Scotia Sea on the outflow of Weddell Sea deep water. *Journal of Marine Research*, **51** (1): 135-153.

Mathiot, P., Goosse, H., Fichefet, T., Barnier, B., and Gallée, H., 2011. Modelling the seasonal variability of the Antarctic Slope Current. *Ocean Science*, **7** (4): 445-532.

Moffat, C., Owens, B., and Beardsley, R. C., 2009. On the characteristics of Circumpolar Deep Water intrusions to the west Antarctic Peninsula Continental Shelf. *Journal of Geophysical Research*, **114** (C5), DOI: 10.1029/2008JC004955.

Naveira Garabato, A. C., Heywood, K. J., and Stevens, D. P., 2002. Modification and pathways of Southern Ocean Deep Waters in the Scotia Sea. *Deep Sea Research Part I: Oceanographic Research Papers*, **49** (4): 681-705, DOI: 10.1016/S0967-0637(01)00071-1.

Nowlin, W. D., and Klinck, J. M., 1986. The physics of the Antarctic Circumpolar Current (paper 6R0315). *Reviews of Geophysics*, **24** (3): 469.

Nowlin, W. D., and Zenk, W., 1988. Westward bottom currents along the margin of the South Shetland Island Arc. *Deep Sea Research Part A. Oceanographic Research Papers*, **35** (2): 269-301.

Orsi, A. H., Iii, T. W., and Jr, W. D. N., 1995. On the meridional extent and fronts of the Antarctic Circumpolar Current. *Deep Sea Research Part I*: *Oceanographic Research Papers*, **42** (5): 641-673.

Peña-Molino, B., McCartney, M. S., and Rintoul, S. R., 2016. Direct observations of the Antarctic Slope Current transport at 113°E. *Journal of Geophysical Research: Oceans*, **121**: 7390-7407, DOI: 10. 1002/2015JC011594.

Padman, L., Fricker, H. A., Coleman, R., Howard, S., and Erofeeva, L., 2002. A new tide model for the Antarctic ice shelves and seas. *Annals of Glaciology*, **34** (1): 247-254.

Quetin, L. B., and Ross, R. M., 1984. Depth distribution of developing *Euphausia superba* embryos, predicted from sinking rates. *Marine Biology*, **79** (1): 47-53.

Quetin, L. B., and Ross, R. M., 1984. School composition of the Antarctic krill *Euphausia superba* in the waters west of the Antarctic Peninsula in the austral summer of 1982. *Journal of Crustacean Biology*, **4** (5): 96-106.

RDI, 1989. *Acoustic Doppler Current Profilers Principles of Operation–A Practical Primer: RD Instruments*. San Diego, Calif., 36pp.

Ross, R. M., Hofmann, E. E., and Quetin, L. B., 2013. *Water Mass Distribution and Circulation West of the Antarctic Peninsula and Including Bransfield Strait*. American Geophysical Union.

Savidge, D. K., and Amft, J. A., 2009. Circulation on the West Antarctic Peninsula derived from 6 years of shipboard ADCP transects. *Deep Sea Research Part I: Oceanographic Research Papers*, **56** (10): 1633-1655.

Selph, K. E., Apprill, A., Measures, C. I., Hatta, M., Hiscock, W. T., and Brown, M. T., 2013. Phytoplankton distributions in the Shackleton Fracture Zone/Elephant Island region of the Drake Passage in February−March 2004. *Deep Sea Research Part II: Topical Studies in Oceanography*, **90**: 55-67, DOI: 10.1016/j.dsr2.2013.01.030.

Shi, J., Sun, Y., Jiao, Y., Hao, G., Wang, M., 2016. Water masses and exchanges in the region around the northern tip of the Antarctic Peninsula observed in summer 2011/2012. *Chinese Journal of Polar Research*, **28** (1): 67-79 (in Chinese).

Siegel, V., Reiss, C. S., Dietrich, K. S., Haraldsson, M., and Rohardt, G., 2013. Distribution and abundance of Antarctic krill (*Euphausia superba*) along the Antarctic Peninsula. *Deep Sea Research Part I: Oceanographic Research Papers*, **77**: 63-74, DOI: 10.1016/j.dsr.2013.02.005.

Stewart, A. L., and Thompson, A. F., 2015. Eddy-mediated transport of warm Circumpolar Deep Water across the Antarctic Shelf Break. *Geophysical Research Letters*, **42** (2): 432-440, DOI: 10.1002/2014GL062281.

Stewart, A. L., and Thompson, A. F., 2016. Eddy generation and jet formation *via* dense water outflows across the Antarctic continental slope. *Journal of Physical Oceanography*, DOI: 10.1175/JPO-D-16-0145.1.

Thompson, A. F., Heywood, K. J., Thorpe, S. E., Renner, A. H., and Trasviña, A., 2009. Surface circulation at the tip of the Antarctic Peninsula from drifters. *Journal of Physical Oceanography*, **39** (1): 3-26.

Youngs, M. K., Thompson, A. F., Flexas, M. M., and Heywood, K. J., 2015. Weddell sea export pathways from surface drifters. *Journal of Physical Oceanography*, **45** (4): 1068-1085, DOI: 10.1175/JPO-D-14-0103.1.

Zhou, M., Zhu, Y., Dorland, R. D., and Measures, C. I., 2010. Dynamics of the current system in the southern Drake Passage. *Deep Sea Research Part I: Oceanographic Research Papers*, **57** (9): 1039-1048.

Zhou, M., Zhu, Y., Measures, C. I., Hatta, M., Charette, M. A., Gille, S. T., Frants, M., Jiang, M., and Mitchell, B. G., 2013. Winter mesoscale circulation on the shelf slope region of the southern Drake Passage. *Deep Sea Research Part II: Topical Studies in Oceanography*, **90**: 4-14.

(Edited by Ji Dechun)